

# DAVIDSON LABORATORY

Letter Report 1332



DD  
FORM  
JAN 23 1969  
R  
C

TESTS OF A  
VARIABLE SWEEP HYDROFOIL  
WITH CAVITATION AND VENTILATION

by

John A. Mercier

January, 1969



STEVENS INSTITUTE  
OF TECHNOLOGY  
CASTLE POINT STATION  
HOBOKEN, NEW JERSEY

This document has been approved  
for public release and sale; its  
distribution is unlimited.

Distribution of this document is unlimited

**DAVIDSON LABORATORY**

**Letter Report #1332**

**January 1969**

**TESTS OF A  
VARIABLE SWEEP HYDROFOIL WITH CAVITATION AND VENTILATION**

**by**

**John A. Mercier**

**'Prepared for the  
Department of the Navy  
Naval Air Systems Command  
Contract N600(19)62908, Task Order 10  
(DL Project 3374/310)**

**Distribution of this document is unlimited. Application for copies may be made to the Defense Documentation Center, Cameron Station, 5010 Duke Street, Alexandria, Virginia 22314. Reproduction of the document in whole or in part is permitted for any purpose of the United States Government.**

**Approved:**

*S. Tsakonas*

**Stavros Tsakonas, Chief  
Fluid Dynamics Division**

**v + 20 pages  
13 figures**

## ABSTRACT

An experimental study of the performance of a variable sweep hydrofoil was carried out in the Davidson Laboratory variable pressure circulating water channel under conditions of reduced ambient pressure. A hydrofoil with tapered planform and typical sub-cavitating sections in the high aspect ratio (AR) attitude was attached to a base ventilated strut in such a way that it could be rotated, thus changing foil sweep. The attack angle of the foil and strut system were adjustable.

Measurements were made of the lift and drag acting on the foil and strut as a function of attack angle, sweep angle, depth of submergence and cavitation index for both steady foil position and with sweep and attack angles continuously varying. Still and motion picture records of some interesting flow phenomena were obtained.

## KEYWORDS

Hydrofoils  
Variable Sweep

TABLE OF CONTENTS

	iii
INTRODUCTION . . . . .	1
<b>MODEL AND APPARATUS</b> . . . . .	<b>3</b>
TEST PROCEDURE <b>AND</b> PROGRAM . . . . .	7
RESULTS . . . . .	9
DISCUSSION . . . . .	16
CONCLUSIONS . . . . .	18
<b>RECOMMENDATIONS</b> . . . . .	<b>18</b>
REFERENCES . . . . .	19
<b>APPENDIX</b> . . . . .	<b>21</b>
FIGURES (1-13)	

## INTRODUCTION

Variable sweep hydrofoils may be useful for applications to hydrofoil craft and sea-based aircraft. In the case of the hydrofoil craft, it may be possible to vary the foil's aspect ratio, sweep and attack angle to obtain a most favorable attitude. For any desired speed, craft weight or sea conditions and, hence, provide for most efficient hydrodynamic performance throughout the entire range of operating conditions. For seaplane applications, different foil (or hydro-ski) attitudes can be used so that the impact loads attendant on landing, especially in a seaway, may be minimized while the lift-to-drag ratio may be maximized for take-off. The investigation of variable sweep operation of hydrofoils was recommended by Mr. E.H. Handier, who holds a patent covering this concept.

A previous experimental study of a variable sweep hydrofoil, reported by Mercier,<sup>1</sup> indicated that such systems can be applied without encountering harmful lift or drag discontinuities provided the foil attitude of sweep and attack angle is varied "smoothly." A further finding was that adjustments of aspect ratio, sweep, and attack angle can provide more favorable (in terms of foil lift-to-drag ratio) conditions than a fixed sweep foil system under certain operating conditions. These studies were carried out using a hydrofoil model with an elliptical planform, and tests were conducted in Davidson Laboratory (DL) Towing Tank No. 2. The model and apparatus were attached to the rotating arm at a radius of 31 feet so that the effective flow over the model was representative of straight-line motion.

In these previous tests, the high values of ambient pressure precluded the possibility of studying cavitation of the hydrofoil. Inasmuch as the potential flow discontinuities and consequent lift discontinuities

---

<sup>1</sup> Superior numbers in text matter refer to similarly numbered references which are listed at the end of this report

associated with cavitation and with ventilation are of great importance, the present experimental program was prepared. Measurements were made of both steady-state forces and forces acting while the sweep angle and attack angle are continuously varying. The influence of features such as angle of attack, sweep, sweep rate, cavitation number and depth of submergence were investigated,

Records of the flow about the foil and strut were obtained with 16mm motion pictures for a variety of test runs. An edited copy of this record, with descriptive titles preceding each of the test runs; has been submitted to the contracting agency as a separate appendix to this report. An annotated listing of the tests shown on this film is included in this report as an appendix (page 21).

## MODEL AND APPARATUS

A sketch of the hydrofoil and strut model is shown in Figure 1. The selection of the thin (5 percent thickness ratio) ogival section shape presented for the high aspect ratio sweep attitude was based on its reasonably good cavitation qualities, the relatively small scale effect or Reynold's number dependence of its hydrodynamic characteristics, and the feasibility of accurate manufacture. In the low aspect ratio attitude, where fairly high attack angles ( $\alpha$ ) are likely to be required to achieve the required lift, the foil represents a reasonable foil or hydro-ski shape although some longitudinal camber might be desirable for this case, especially for ventilated or super-cavitating operation. The foil's tapered planform in the high aspect ratio attitude was selected to deliberately promote the occurrence of local flow separation at wing tips prior to its occurrence over the rest of the wing as the angle of incidence is increased. This was done to avoid the possibility of precipitate lift breakdown which might occur if flow separation occurred over the entire foil at the same instant. The possibility of cavitation or ventilation accompanying the separation with greatly reduced pressure (low values of the cavitation index) makes the possible lift-breakdown of greater importance,

The foil "span" (or greatest length) is 6.00 inches. The "wing-tip chord" is 0.6 inches while the mid-span chord is 2.365 inches. Thus, when the wing span is transverse to the flow condition, in the high aspect ratio (AR) condition, the AR is 4.05. This condition is referred to as zero-degree sweep ( $\beta$ ) for the present tests. At the 90 degree sweep attitude, the low AR is 0.629. The foil is made of stainless steel with a thickness-chord ratio (for the high AR position) of 0.05. The leading end trailing edges are filed sharp,

The foil is mounted on what is considered to be a representative high-speed hydrofoil strut. This strut has parabolic sections with a squarely-cut-off base which fixes the separation point of the flow and

and virtually assures ventilation of the strut base at reasonably high speeds. The strut is made of brass and has a chord of 1.2 inches and a base-thickness-to-chord-ratio of 0.20.

The tests were carried out in the Davidson laboratory variable pressure circulating water channel. Figure 2 shows the principal dimensions and general features of this facility. Speeds of around 18 feet per second can be achieved, under atmospheric pressure operation, with reasonably smooth flow containing a fairly small proportion of air bubbles. The pressure above the free water surface can be reduced, using a vacuum pump, to around 0.5 psia, provided all access openings to the tunnel are securely sealed. Under these reduced pressure conditions the maximum test speed is somewhat reduced since gas bubbles entrained in the water will expand greatly at the low pressures. For tests at reduced pressure; it is essential to deaerate the water by running the water channel at a moderate speed for a few hours with the vacuum pump operating. If there are even small air leaks to the inside of the channel, the minimum pressure is increased and the maximum water speed is reduced since deaeration of the water cannot be successfully effected. The problem of bubbles in the flow obscuring observations and altering flow phenomena is increased at high speeds, of course, because of the reduction of pressure which accompanies increased speed, as indicated by Bernoulli's equation. For the present tests, a small air leak to the channel existed but was not detectable or correctable, and the maximum test speed which could be used was limited to around 13.5 feet per second,

The speed is measured by noting the difference in static pressure at the entrance and at the outlet of the nozzle in front of the measuring section, using a differential water manometer. The pressure inside the water channel is indicated by use of a differential mercury manometer to indicate the difference between atmospheric pressure and the pressure above the test section together with a barometer to measure the absolute atmospheric pressure.

The hydrofoil and strut are attached to a system of position adjusting devices and force balances. A photograph of the mounting arrangements is shown in Figure 3. This apparatus with side plates attached is shown

in place, on top of the test section cover in figure 4, which shows the flow channel with the test equipment setup.

The lift and the drag of the foil plus strut system are sensed by the two stiff spring element force balances shown in Figure 3. These balances are similar in design, with a capacity of  $\pm 10$  lbs corresponding to a deflection of .050 inches. The deflection of the springs is detected by a linear variable differential transformer (LVDT) which converts movement to an electrical signal which is transmitted outside of the tunnel by means of sealed wires, and is then amplified and recorded. These balances were calibrated prior to final installation inside the sealed tunnel.

The elevation of the foil system is controlled by the push-rod mount illustrated in Figure 3. The depth of submergence is adjusted by means of the two threaded bolts and nuts. The nominal depth of submergence of the foil is measured from the stillwater level to the flat bottom of the foil when the attack angle setting is zero degrees.

The sweep and attack angle are adjusted by servo-controlled motors. These rotary position controllers are "slaves," which assume the angular orientation of the "master" of the self-synchronous (seisyn) device, which is actuated by the test operator outside the reduced pressure channel. The master elements are shown in the photograph of Figure 5 as part of the apparatus, in the lower left-hand corner of the desk. This apparatus is arranged so that the attack angle and sweep of the foil are related to the  $r$  and  $\theta$  coordinates of a pointer which slides on a pivoting arm. A 90-deg change of the  $\theta$  position of the pointer produces a similar 90-deg change in the sweep angle. A 4-in change in the radial position of the pointer produces a 10-deg change in the attack angle of the foil-strut system.

Attack angle changes are affected by the slave element of the rotary positioner which has an horizontal axis, working through the gear train (shown in Figure 3) and pivoting the system about the axis indicated in that figure. The sweep angle is effected by the other rotary positioner, which is coupled to a 1/8-in diameter shaft which is, in turn, attached to the center of the planform of the hydrofoil. This sweep adjustment

shaft pierces the center of, and is supported by, the strut.

The foil's attitude of sweep and attack angle is sensed by a pair of rotary variable differential transformers (RVDT's). For the attack angle, this device is connected to the foil mounting apparatus inside the flow channel. For the sweep, the RVDT is coupled to the pivoting arm through a gear so that a 90-deg sweep motion produces only 45-deg RVDT motion, which is within the range for a linear output signal. The attack angle transducer is mounted inside the tunnel because of the importance of accurately knowing the foil's instantaneous attack angle. The maximum sweep rate is limited by the speed of the slave elements of the selsyn unit rather than by the rate at which the test operator sweeps the master element, and is about 60 degrees per second.

The transduced signals, representing drag, attack angle and foil sweep, are amplified and recorded on a tight-beam oscillograph to provide records of these quantities as a function of time.

## TEST PROCEDURE AND PROGRAM

The calibration of the lift and drag balances was accomplished prior to final installation inside the sealed tunnel and again after the tests were completed. Both lift and drag calibrations were carried out with a string which is attached to the foil-strut system and which passes over a very-low-friction pulley. Weights are attached to the end of the string to provide known forces and the corresponding amplified signal recorded.

After aligning the foil sweep and attack angle so that the selsyn devices are "in phase," i.e., the zero positions for attack angle and sweep of the foil correspond to the zero positions of the master control apparatus, the position transducer calibration signals were obtained by adjusting the controller settings and recording the corresponding signals. The alignment was done prior to final installation and sealing of the channel, and calibration signals were recorded at various times during the test program - both with the channel open and with it sealed,

Depressurization of the channel was accomplished before beginning of testing by means of a vacuum pump. The water was then substantially de-aerated by running the water channel at moderate speed, with a vacuum pump in operation for a number of hours. It was found that a small air leak into the channel existed which limited the pressure reduction that could be obtained. This, in turn, limited the maximum test speed which could be used without encountering excessive bubbles. Unfortunately, the leak could not be found and it was decided to accept the obtainable pressure of about 64mm of Hg absolute, or about 0.085 of an atmosphere, and to limit the water velocity to 13.5-ft per second,

All tests were conducted with this maximum pressure reduction with changes in cavitation index being accomplished by changing the speed. The vacuum pump was run continuously during testing to maintain the constancy of the reduced pressure in the test channel,

Because of the leak, the pressure inside the channel returned to nearly atmospheric pressure after the apparatus had been left idle overnight. Since the water had been still during this idle time, it did not absorb much air and required only a brief period of de-aeration procedure to be ready to continue testing.

The first series of tests were conducted to obtain steady-state data on the performance of the foil-strut system under various conditions of operations. The parameters which were varied in these tests include depth of submergence, attack angle, sweep, and water velocity.

Upon completing the series of steady-state tests, a number of tests were carried out with continuous variations of the sweep and/or attack angle. These variations were achieved by the test operator who manually adjusted the position of the  $r-\theta$  pointer of the salsyn master device in as smooth a manner as he could. Occasionally, this adjustment would be jerky, rather than smooth. Highly irregular movements of the foil and strut give test results which are not particularly meaningful.

A series of motion picture records were made to demonstrate the functioning of the apparatus and some of the more interesting flow phenomena, such as cavitation, ventilation and tip vortices. An edited version of these observations is being submitted separately and an annotated listing of the tests shown in this film is given in the appendix to this report.

Finally, a sequence of still photographs were made of various test conditions. Two kinds of lighting were tried. In the first, photographs were obtained using a shutter speed of 1/200th-of-a-second and illumination by floodlight. In this case the bubbles which travel with the flow in the channel appear as streaks approximately  $\frac{1}{2}$ -inch in length. Additional photographs were taken with electronic flash illumination, having a duration of about 1/1000th-of-a-second, for which case the individual bubbles in the flow show up rather clearly.

## RESULTS

All of the steady-state test runs have been analyzed and data from some of these tests will be presented to demonstrate the kind of performance which was obtained with this hydrofoil.

Lift coefficients as a function of attack angle in the high AR configuration are shown in Figure 6 for tests at three different nominal depths of submergence. The lift coefficient is defined as

$$C_L = \frac{\text{Lift, lb}}{\frac{\rho}{2} A v^2}$$

where  $\rho$  is the fluid mass density,  $\text{lb-sec}^2/\text{ft}^4$ ;  $A$  is the foil's planform area,  $.0617 \text{ ft}^2$ ; and  $v$  is the speed of the water in the channel,  $\text{ft/sec}$ . The water temperature for these tests was  $74^\circ\text{F}$  and did not fluctuate by more than  $2^\circ\text{F}$  during the course of the experimental work. These tests were carried out with water velocity of  $11.80 \text{ ft/sec}$  with cavitation indices as exhibited in the figure.

Cavitation index is defined as

$$\sigma = \frac{p_a - p_v}{\frac{\rho}{2} v^2}$$

where  $p_a$  is the ambient pressure in the stream at a depth corresponding to the nominal hydrofoil submergence depth,  $\text{lb/ft}^2$ , and  $p_v$  is the vapor pressure of water corresponding to the measured water temperature,  $\text{lb/ft}^2$ . The Reynolds number for these tests, equal to  $v \times \text{mean chord} / \nu$ , where  $\nu$  is the kinematic viscosity, is  $1.46 \times 10^5$ . For tests at the same speed, in the low aspect ratio attitude, the Reynolds number based on the span length is  $5.91 \times 10^5$ .

The results presented in Figure 6 reveal differences in lift curve slope and zero-lift angle, as shown in Table 1 on the following page.

TABLE 1

DATA ANALYSIS  
High Aspect Ratio (Figure 6)

Test-Run	Nominal Depth of Submergence (d, inches)	d/mean chord	Cavitation Index ( $\sigma$ )	Zero Lift Angle (deg)	Lift Curve Slope (1/deg)
ii	1	0.675	0.908	-1.05	.0586
1	2	1.35	0.955	-0.20	.0620
6	3	3.025	0.985	-0.25	.0643

Low Aspect Ratio (Figure 7)

12	1	0.675	0.908	+0.9	.020
2	2	1.35	0.955	+4.8	.020
7	3	3.025	0.985	+2.5	.020

For the higher aspect ratio, a theoretical lift curve slope for fully wetted wings of .0679 can be derived from a formula given by Jones and Cohen,\* viz.,

$$\frac{\partial c_L}{\partial \alpha} \approx \frac{2\pi AR}{p AR+2} \times \frac{1}{57.3} \quad , \quad \text{per degree}$$

where  $p$  is the ratio of the semiperimeter of the wing to its span. The change in lift curve slope with depth of submergence is in agreement with the trend indicated by hydrofoil theory. The differences in zero-lift angle cannot, unfortunately, be explained in terms of theory. Two-dimensional section theory for finite depth of submergence, as presented by Bernicker,<sup>3</sup> suggests that the zero-lift angle should increase with proximity to the free surface. The influence of the support strut has been studied theoretically by Huang,<sup>4</sup> who finds that its effect on lift should be negligible for reasonably high aspect ratio hydrofoils. The significant zero-lift differences shown in Figure 6 and Table 1 are

not readily explainable but are probably associated with a zero-shift in the electronic instrumentation occurring from run to run. The flow over the hydrofoil surface is non-cavitated except for very slight leading edge bubble cavitation on the outboard sections of the foil which does occur for large attack angles. The wing-tip vortices, trailing aft of the foil, are cavitated - especially when the attack angle is large and the vortex strength is great. These cavitated vortices, which do not connect with the free surface for any of the conditions illustrated in Figure 6, appear to have diameters of about 1/8-inch for the highest lifts and lengths extending beyond the end of the test section.

Data for lift coefficient as a function of angle of attack for the low aspect ratio attitude are exhibited in Figure 7 and Table 1. The lift curve slope for all three of the tests is roughly .020 per degree, which compares with a theoretical value of  $\pi AR/2 \times 57.3 = 0.017$  per degree, for a deeply submerged low aspect ratio hydrofoil. The zero-lift angles again show anomalous differences which may be due to zero-shifts in the electronic apparatus between runs. The non-linear dependence of lift on attack angle is clearly evident in the figure. The discontinuous change in the lift coefficient for the 1-inch depth of submergence, which occurs for an attack angle of 11.5 degrees, is associated with sudden ventilation, or the bursting connection of the wing-tip vortices with the atmosphere over the free surface. At lower attack angles the wing-tip vortices, which originate at the sharp leading edge corners of the low aspect ratio hydrofoil, are not connected with the free surface and have a size which varies with the intensity of the vorticity.

Photographs which illustrate the nature of the flow for the high and low aspect ratio foil attitudes are shown in Figure 8. These pictures were obtained using electronic flash illumination having a duration of about 0.001 second.

The effect of water speed on the lift curve slope was evaluated for the high end low aspect ratio attitudes for the nominal depth of submergence of 1 inch (depth/mean chord = 0.675). Table 2 presents the results of this study, and also notes the angle for which ventilation occurs.

TABLE 2

## EFFECT OF SPEED ON LIFT CHARACTERISTICS

Run No, AR	V ft/sec	$\sigma$	$\partial C_L / \partial \alpha$ 1/deg	$\alpha_{vent}$ deg
16 4.05	8.16	1.90	0.0628	over 12
19 4.05	9.97	1.272	0.0600	over 12
11 4.05	11.80	0.908	0.059%	over 12
24 4.05	13.36	0.708	0.0598	$\approx 11.5$
17 0.629	8.16	1.90	0.021	over 14
20 0.629	9.97	1.272	0.020	-12.0
12 0.629	11.80	0.908	0.020	$\approx 11.5$
25 0.629	13.36	0.708	0.0195	$\approx 10$

Although some cavitation did occur on the hydrofoils for large angles of attack and the higher speed, its extent was slight and it probably was not sufficient to have an appreciable effect on the lift. The differences in lift rates for the tests at different speeds may be associated with a Reynolds number influence, although the accuracy of the data is not adequate to clearly determine this effect.

No numerical values for the precision of the data were derived from such procedures as repeated readings. It is the author's opinion, however, based on the ability to resolve the oscillogram records and on the consistency of the data for a given run, that the lift values obtained are mostly within  $\pm 0.2$  lb of the correct relative value. This does not include the deviation which may be associated with zero-level shifts which may account for as much as 0.5-lb error, and which is nearly constant for the duration of a test run and, hence, does not affect the determination of lift rates, it may be noted that the significant zero level shifts occurred during the first sequences of tests

conducted and that the apparatus behaved more uniformly for the later tests where the absolute values of the lift are reliable within approximately the  $\pm 0.2$  which has been previously noted. The drag force measurements were not subject to this serious zero-shift problem. These are felt to be reliable within about  $\pm 0.10$  lb. For a stream speed of 11.8 ft/sec, the lift coefficient may be considered accurate to within  $\pm 0.023$  and the drag coefficients may be considered accurate to within  $\pm 0.011$ . The accuracy of the coefficients is, of course, poorer for lower speeds. The use of faired results, plotted against  $\alpha$  and/or  $\beta$ , improves confidence in the data presented.

A polar diagram of lift coefficient versus drag coefficient of the foil and strut combination at different sweep angles and attack angles is given in figure 9 for a foil nominal depth/mean chord ratio of 0.675. The optimum sweep and attack angle can be determined from this chart for a given lift coefficient. It will be seen that the least drag coefficient for this foil-strut-depth combination corresponds to zero sweep angle for values of lift coefficient greater than about 0.18. Below this value a slight improvement in performance can be obtained by adopting a different sweep angle. In the previous tests, reported in Reference 1, where the lift and drag of the hydrofoil were measured but not including the strut forces, it appeared that foil sweep would be advantageous even for lift coefficients over 0.3. This feature, of optimum attitude, will be a function of foil and strut design as well as of the 'accounting' system used, e.g., whether the forces acting on the foil alone or those on the foil-strut combination are measured. The best lift-drag ratio obtained for the present combination, as shown in Figure 9, is 6.67, for values of  $C_L$  around 0.4.

The effect on lift of unsteadiness due to continuous variation of the attack angle, for the high AR attitude and depth of 2 inches, is shown in Figure 10 along with the corresponding curve for steady-state tests taken from Figure 6. The rate of change of  $\alpha$  is not uniform during the unsteady tests because the manual adjustment of the servo-position controller by the test operator cannot be achieved with great smoothness. For the average rates shown in Figure 10, of 1.81 deg/sec

and 3.29 deg/sec, the rates actually varied from 1.1 to 3.2 deg/sec, and from 2.0 to 4.8 deg/sec, respectively. These average rates, for the test speed of 11.72 ft/sec, correspond to achieving a 10 deg attack angle change while the foil and strut traverse a distance corresponding to 130 foil spans for the lower rate and 71 foil spans for the higher rate. It is apparent that for these fairly low rates of change of  $\alpha$ , the unsteadiness does not have an appreciable effect on the lift.

The effect of unsteadiness due to sweep is illustrated in Figure 11, when  $C_L$  and  $10C_D$  are given as a function of  $P$  for three different rates of sweep, 12.3 deg/sec, 12.9 deg/sec and 18.4 deg/sec. Again, the unsteadiness does not have a significant effect,

A series of tests were conducted in which the attack angle and sweep were varied simultaneously, Figure 12 gives the results of lift measurements for two of these tests, for which the average sweep rates were around 10 deg/sec. In one case,  $\alpha$  varies from 2 deg to 7 deg as the sweep varied from high AR to low AR attitude, and the lift coefficient curve varies smoothly, For the case of  $\alpha$  changing from 3 deg to 11 deg, the lift breaks down precipitately for  $\beta$  about 70 deg, due to ventilation, It was noted for many of the test sequences that ventilation would occur during the process of sweeping the foil for lower values of  $\alpha$  than for the case of  $\beta = 90$  deg. For example, for the speed at which the tests shown in Figure 12 were conducted, 13.44 ft/sec, the angle of attack for ventilation in the 90-deg sweep attitude was 10 deg, whereas ventilation occurred for test run 82 at  $\alpha \approx 9.2$  deg and  $\beta \approx 70$  deg. It appears that foil symmetry is advantageous in delaying inception of ventilation, From a number of observations, this lift-breakdown phenomena appeared to be independent of whether the foil's sweep and attack angle were continuously varying or changed very gradually, in discrete steps. It may be noted that tests were conducted where, after the attack angle and sweep were fixed, the flow would persist unventilated for a while and then suddenly burst into the fully ventilated condition. The ventilated flow condition is basically stable and will not revert to non-ventilated behavior unless the lift coefficient is greatly reduced.

One reason for carrying out the tests illustrated in Figure 12 was

to see whether, by varying sweep and attack jointly, a relatively uniform lift coefficient could be obtained over the cycle, This was not achieved, and it is clear that it cannot be done for even moderate values of lift coefficient without risking the occurrence of calamitous lift-breakdown due to ventilation, for high speeds and low depths of submergence.

Motion pictures of certain conditions of operation were recorded and a copy of the edited film has been submitted to the contracting agency . The appendix of this report lists the conditions illustrated and notes some of the phenomena of interest which are to be observed in this film.

Two still photos which are thought to be of interest are shown in Figure 13. Illustration 13-a shows the ventilated region behind the strut being pinched-off by a line of solid water which can be seen about one-third of the distance down the strut, This pinch-off instability progresses down the strut to the bottom and has been observed in many of the tests, particularly at relatively low speeds and moderate attack angles. This phenomenon can be detected in film sequence 6 of the motion picture. Figure 13-b shows the large, spiralling wing-tip vortices which may occur, without ventilation, for high attack angles and not too shallow depth of submergence In the low aspect ratio attitude, This is also shown clearly in film sequence 8 of the motion picture.

## DISCUSSION

The effect of unsteadiness due to continuous variations of foil sweep and attack angle do not have an important effect on the forces acting on the foil-strut system according to the present test results, even for the case of ventilation inception. The occurrence of ventilation does have a very important effect, however, especially on the lift coefficient.

Test results for non-ventilated flow exhibit reasonable lift curve slopes for tests in the high and low aspect ratio condition and for various depths of submergence. The lift curve slopes given in table 3 for tests in the high aspect ratio ( $AR \approx 4.05$ ) attitude are compared in Table 3 with theoretical lift curve slopes for two-dimensional hydrofoils near the free surface, as discussed by Bernicker.<sup>3</sup>

TABLE 3

THEORETICAL AND EXPERIMENTAL DEPENDENCE OF  
LIFT CURVE SLOPE ON DEPTH OF SUBMERGENCE

depth/mean chord d/c	$\frac{\text{(theoretical slope)}}{\text{(theor. } \infty \text{ depth slope)}}$ [Ref. 3, Fig. 2]	$\frac{\text{(theor. slope)}}{\text{(theor. slope for } d/c=2.025)}$	$\frac{\text{(exper. slope)}}{\text{(exper. slope for } d/c=2.025)}$ [from Table 3]
0.675	0.900	0.913	0.912
1.35	0.970	0.984	0.965
2.025	0.986	1.00	1.00

The correlation is seen to be reasonably good.

Lift versus drag characteristics show that the most favorable sweep angle for this hydrofoil-strut system is 0 deg for values of lift coefficient above 0.18. Only a slight improvement in performance

over this attitude can be achieved by sweeping the foil for the lower values of  $C_L$ . Previous tests, reported in Reference 1, where the forces on the foil alone were measured, indicated that sweep could have a significant effect on lift-to-drag ratio over a wider range of  $C_L$  values. The particular foil-strut combination studied will affect the optimum attitude characteristics,

Cavitation index was varied by varying the water speed, but was not extended to very low values because the pressure in the test section could not be reduced to sufficiently low values. The lowest value reached,  $\sigma = 0.71$ , corresponds to a full-size speed of about 33 knots, under atmospheric pressure plus 2-ft of sea water head. The angle of attack for which ventilation inception occurs was found to be a function of cavitation index, or speed, as is shown in Table 4 for a depth/mean chord ratio of 0.675. For greater depths, the required attack angle for ventilation is substantially greater. For example, for low aspect ratio,  $d/c=0.675$ ,  $v = 11.80$ , the inception angle is 11.5 deg, while for the same speed and  $d/c = 1.35$ , ventilation will not occur even for attack angles up to 14 deg (see Figure 13). The effect of ventilation, which occurs suddenly, is to produce a very large instantaneous reduction of lift, while increasing the extent of cavitation, unconnected with the free surface, produces gradual changes (reductions) in lift-curve slope.

A possible application of this variable sweep hydrofoil support system may be for aiding in take-off and landing of sea-based aircraft. For this purpose, the foil would be set at the low aspect ratio attitude for landing, to alleviate impact loads on the craft - especially in rough seas. For take-off, the most efficient high aspect ratio foil attitude would be more favorable. It is not clear whether the variable-sweep, variable attack angle feature would be useful for this application, or if a two-position foil control is adequate, but that may be revealed by a design study for a particular application.

## CONCLUSIONS

1. Rotatable variable sweep hydrofoils can be used without encountering harmful lift or drag discontinuities due to smooth variations in attitude, provided ventilation of the foil is avoided.
2. Foil performance, including forces and ventilation inception, is not influenced by the unsteadiness associated with changes in attitude at the relatively slow rates which were used for the present study,
3. Lift versus drag characteristics for a hydrofoil-strut system are affected by the sweep and attack angle. For low values of  $C_L$ , a more favorable sweep angle than the high AR attitude may be selected but whether this is significant in terms of either range of CL or achievable gains will depend on the particular foil system studied,

## RECOMMENDATIONS

Design studies of foil configurations for various types of craft, including especially a sea-based airplane, should be carried out to assess suitable high and low speed (low and high aspect ratio, respectively) foil configurations. The relative effectiveness of the rotatable foil feature could be judged for various functional requirements. Consideration should be given to the range of anticipated loads and speeds, to cavitation and ventilation liability, structural design features and to mechanical design of the rotating mechanism,

REFERENCES

9. MERCIER, J.A., "Force Measurements on a Rotating Variable Sweep Hydrofoil." Davidson Laboratory Letter Report No. 9980, November 1966.
2. JONES, R.T. and COHEN, D., "High Speed Wing Theory." Princeton University Press, 1957.
3. BERNICKER, R.P., "A Linearized Two-Dimensional Theory for High-Speed Hydrofoils Near the Free Surface." Journal of Ship Research, Vol. 90, No. 9, March 1966.
4. HUANG, T.T., "Strut-Induced Downwash." Hydronautics, Inc. Technical Report 463-7, September 1965.

TESTS OF A VARIABLE SWEEP HYDROFOIL  
IN A CIRCULATING WATER CHANNEL WITH REDUCED PRESSURE

Film Sequence	Water Speed ft/sec	Cavitation Index	Sweep Angle deg	Attack Angle deg	Remarks
<u>TEST SERIES WITH Z-INCH DEPTH BELOW WATER SURFACE</u>					
1	8.24	1.88	0 to 90	+8	Sequences 1-5 illustrate the operation of the sweep and attack angle varying mechanisms Note wing tip vortices (w.t.v.'s) Note w.t.v.'s & leading edge bubble cavitation Note w.t.v.'s
2	10.03	1.27	0 to 90	+8	
3	11.70	0.94	0 to 90	+8	
4	13.44	0.71	0 to 90	+8	
5	11.70	0.94	0	-2 to +14	
<u>NOTE CHANGE IN VIEW OF HYDROFOIL</u>					
6	8.24	1.86	90	-2 to +14	Note slight instability of vented region behind strut
7	10.03	1.27	90	-2 to +14	Note w.t.v.'s
8	11.70	0.93	90	-2 to +14	Note large, spiralling w.t.v.'s
9	13.44	0.70	90	-2 to +14 to -2	Cavitated w.t.v.'s connect to surface (ventilation)
10	8.24	1.86	0 to 90	+2 to +7	Sequences 10-13 illustrate combined sweep and attack angle variation which gives small variations in lift.
11	10.03	1.26	0 to 90	+2 to +7	
12	11.70	0.93	0 to 90	+2 to +7	
13	13.44	0.70	0 to 90	+2 to +7	
<u>TEST SERIES WITH I-INCH FOIL DEPTH BELOW WATER SURFACE</u>					
14	11.70	0.88	0	-2 to +14 to -2	Note distortion of water surface
15	10.03	1.20	90	-2 to +14 to -2	Note precipitation ventilation of upper foil surface
16 q	11.70	0.88	90	-2 to +14 to -2	Sequences 15-17 illustrate that speed has some effect on ventilation inception
17	13.44	0.67	90	-2 to +14 to -2	
18	8.24	1.77	0 to 90	+10	Note leading edge bubble cavitation at sweep $\approx$ 60 degrees
19	10.03	1.20	0 to 90	+10	Ventilates for sweep $\approx$ 30 deg, illustrates ventilation in high AR position
20	11.70	0.88	0 to 90 to 0	+10 to -2	
21	13.44	0.66	0 to 90 to 0	+9.5	Note w.t.v.'s instability at sweep $\approx$ 75 deg

NOTE: Photographed at 24 frames-per-second  
May be projected at either 24 or 16 frames-per-second  
Projection time at 16 frames-per-second is 12 min 30 sec

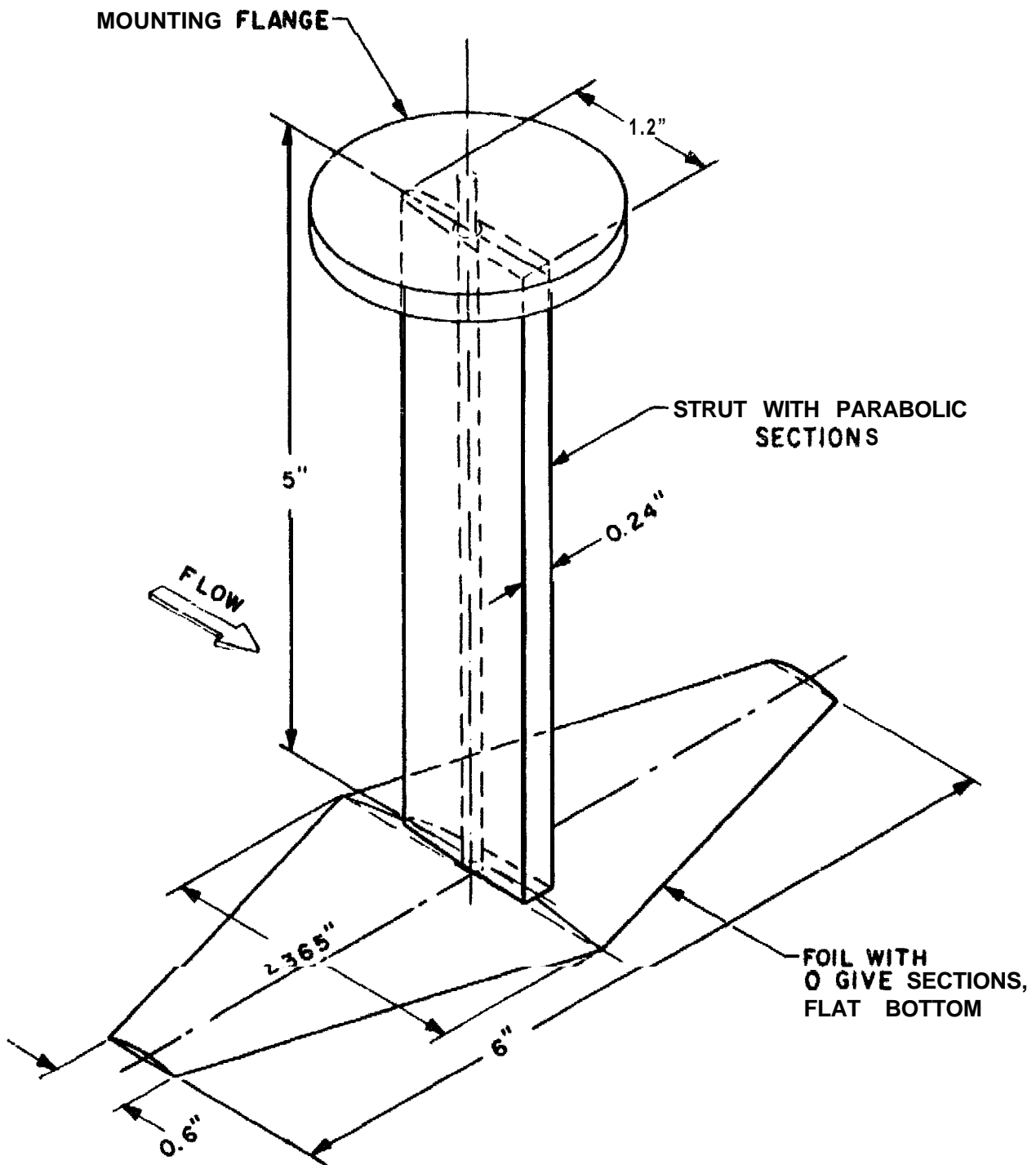
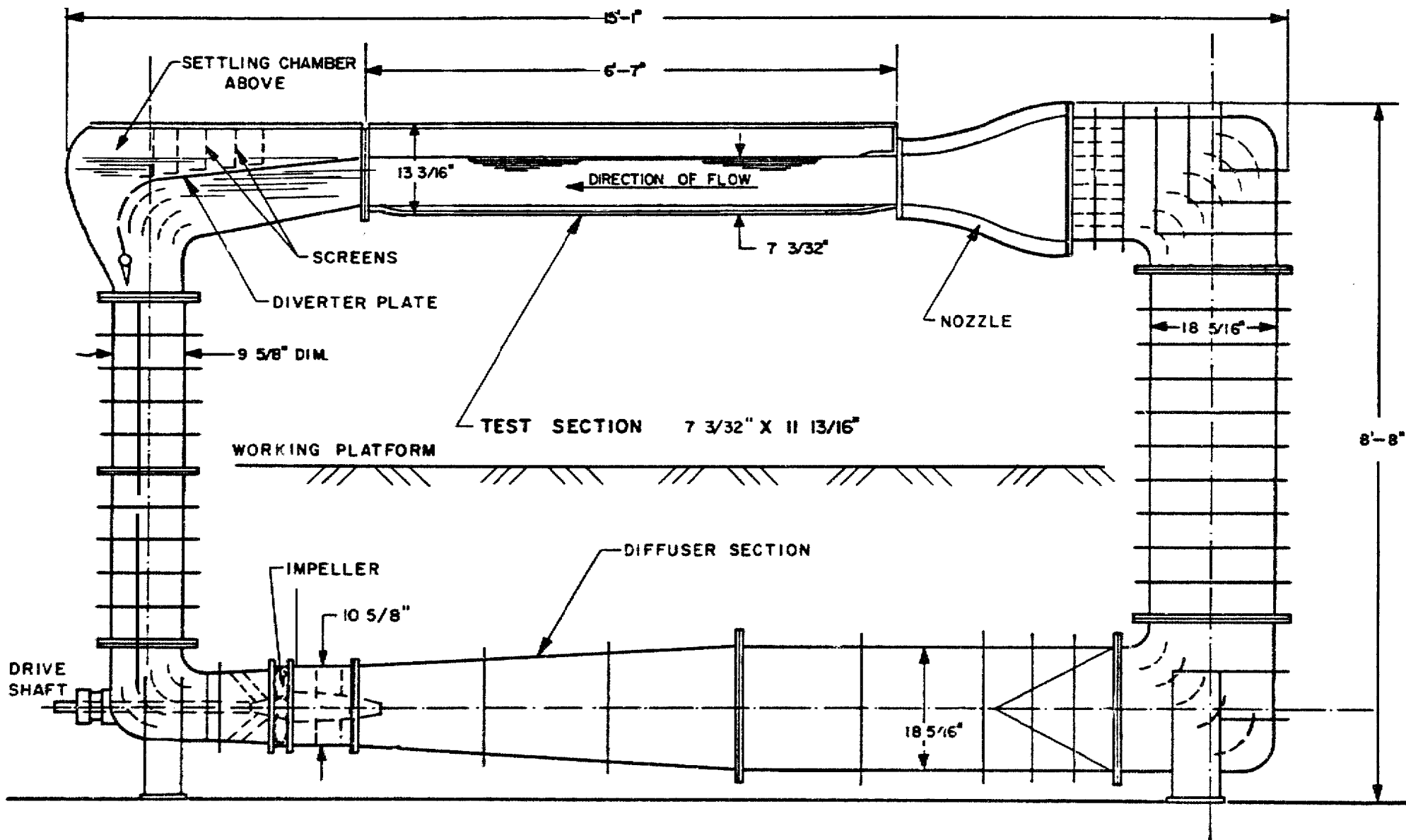


FIG. 1, SKETCH OF HYDROFOIL AND STRUT MODEL  
(LOW  $\alpha$  ATTITUDE SHOWN)



LR-1332

FIG. 2. DAVIDSON LABORATORY VARIABLE PRESSURE CIRCULATING WATER CHANNEL

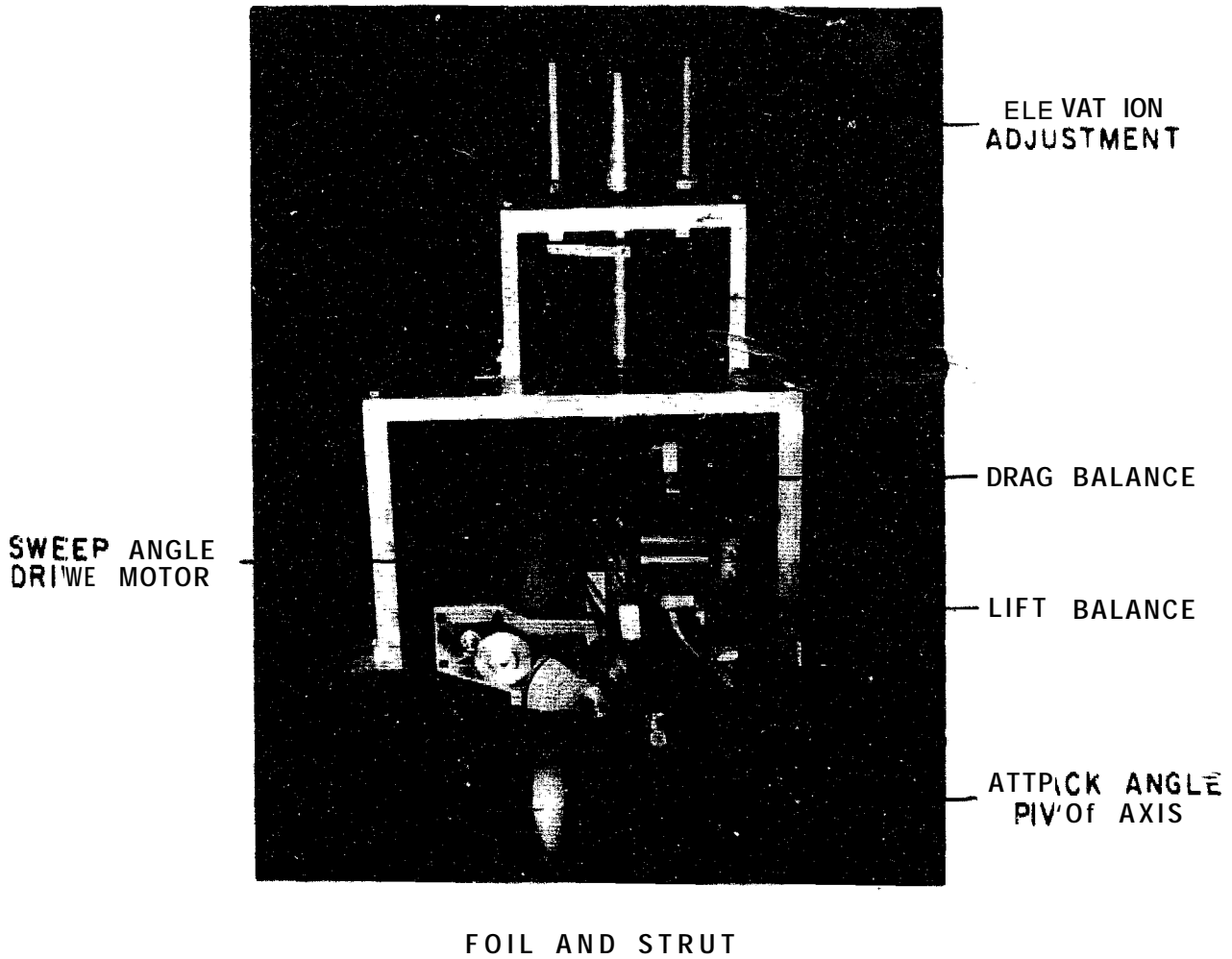


FIG. 3. PHOTOGRAPH OF HYDROFOIL, STRUT, FORCE BALANCES AND POSITIONING APPARATUS

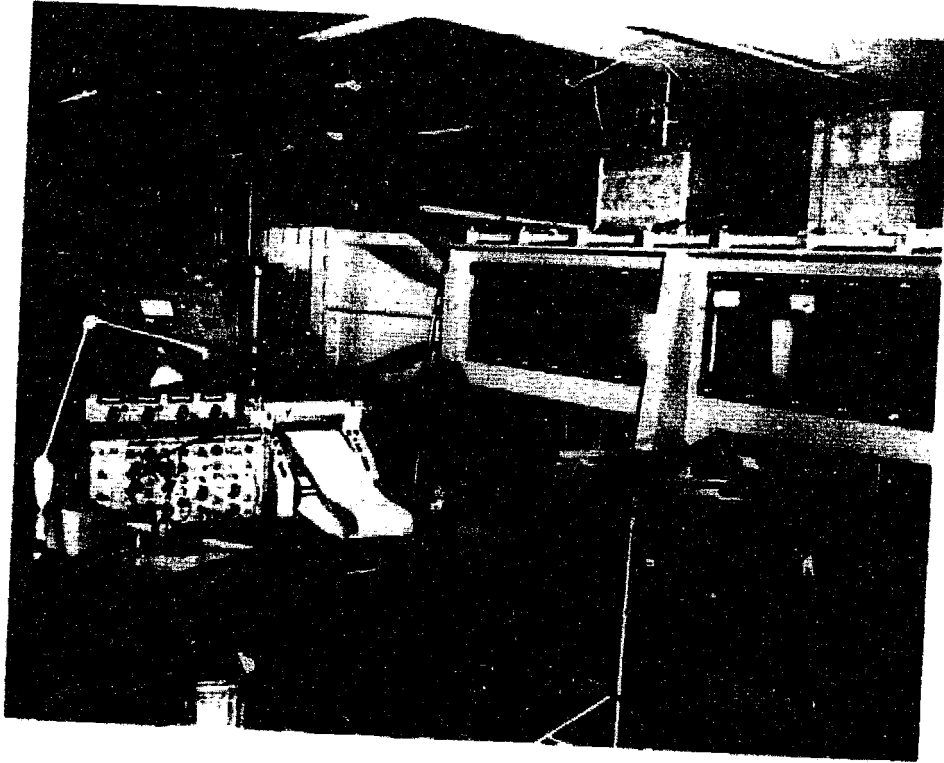


FIG. 4. ILLUSTRATING FLOW CHANNEL, CONTROLS AND RECORDING APPARATUS

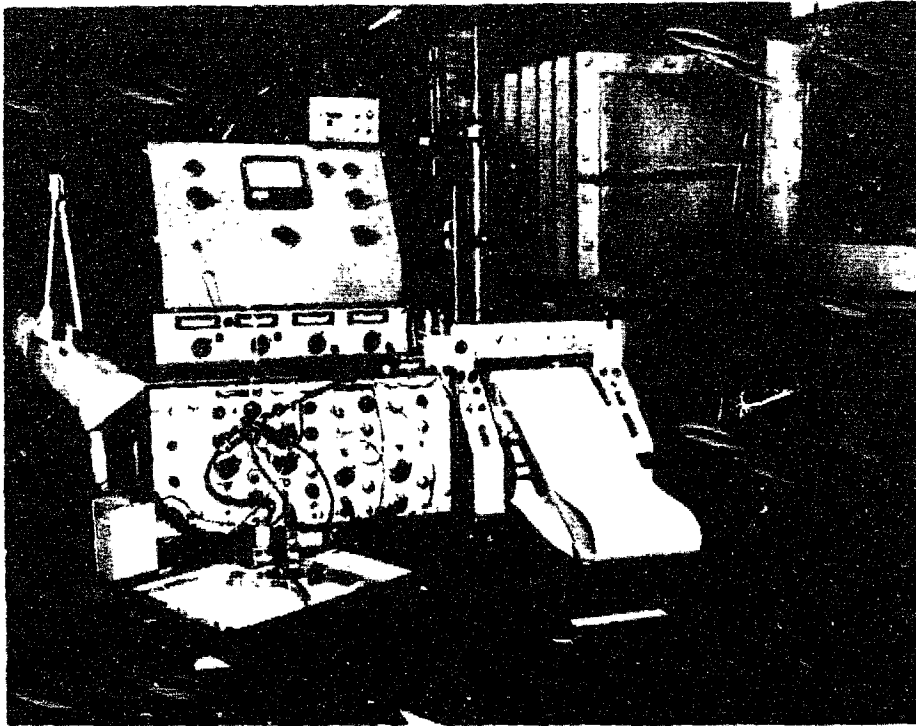
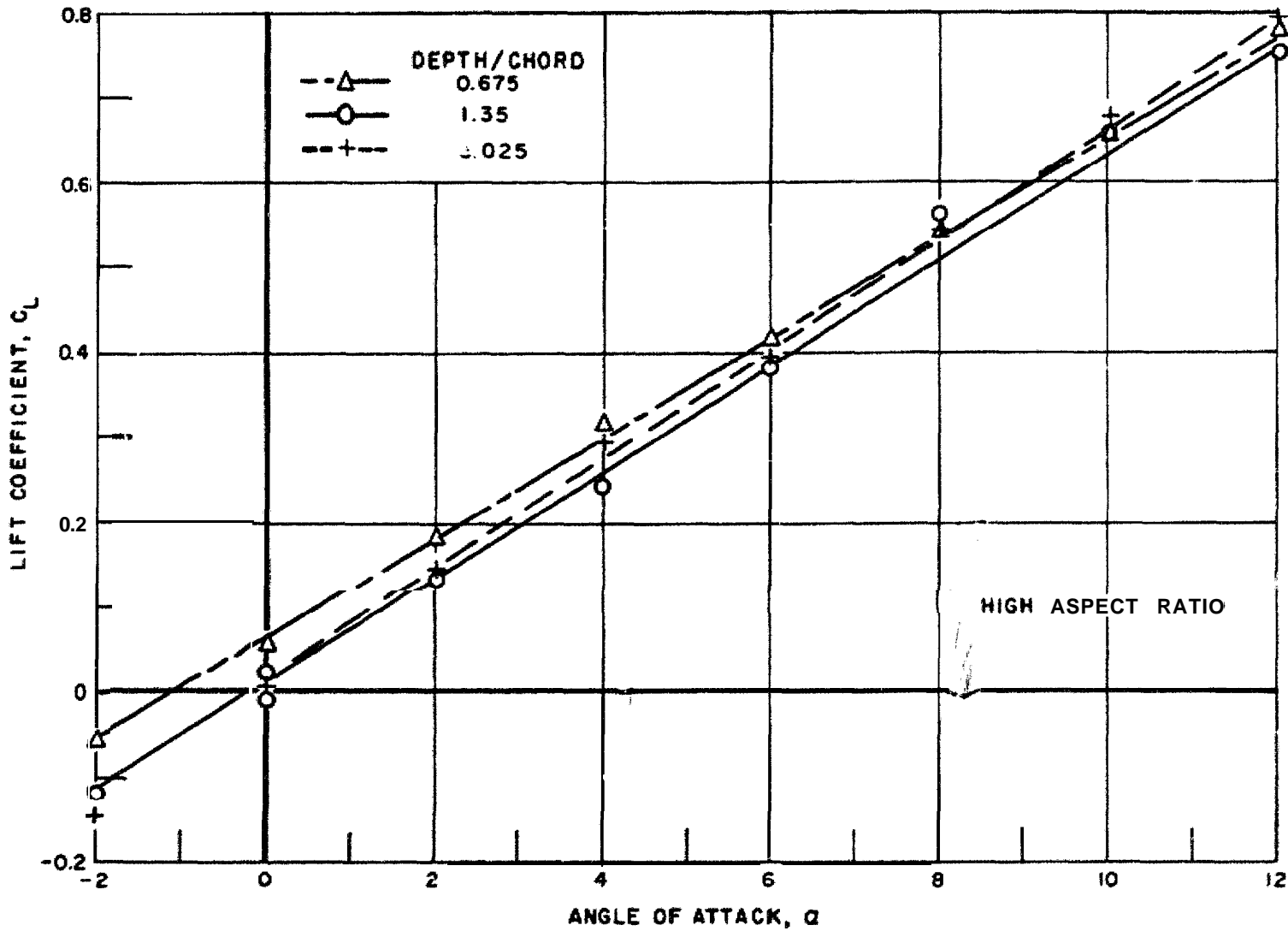


FIG. 5. CONTROLS AND RECORDING APPARATUS, WITH FOIL SWEEP AND ATTACK ANGLE CONTROLLER ON LOWER LEFT-HAND CORNER OF DESK



LR-1332

FIG. 6. EFFECT OF FOIL DEPTH OF SUBMERGENCE ON LIFT. SWEEP ANGLE=0 DEG.  
 $V=11.80$  FT/SEC

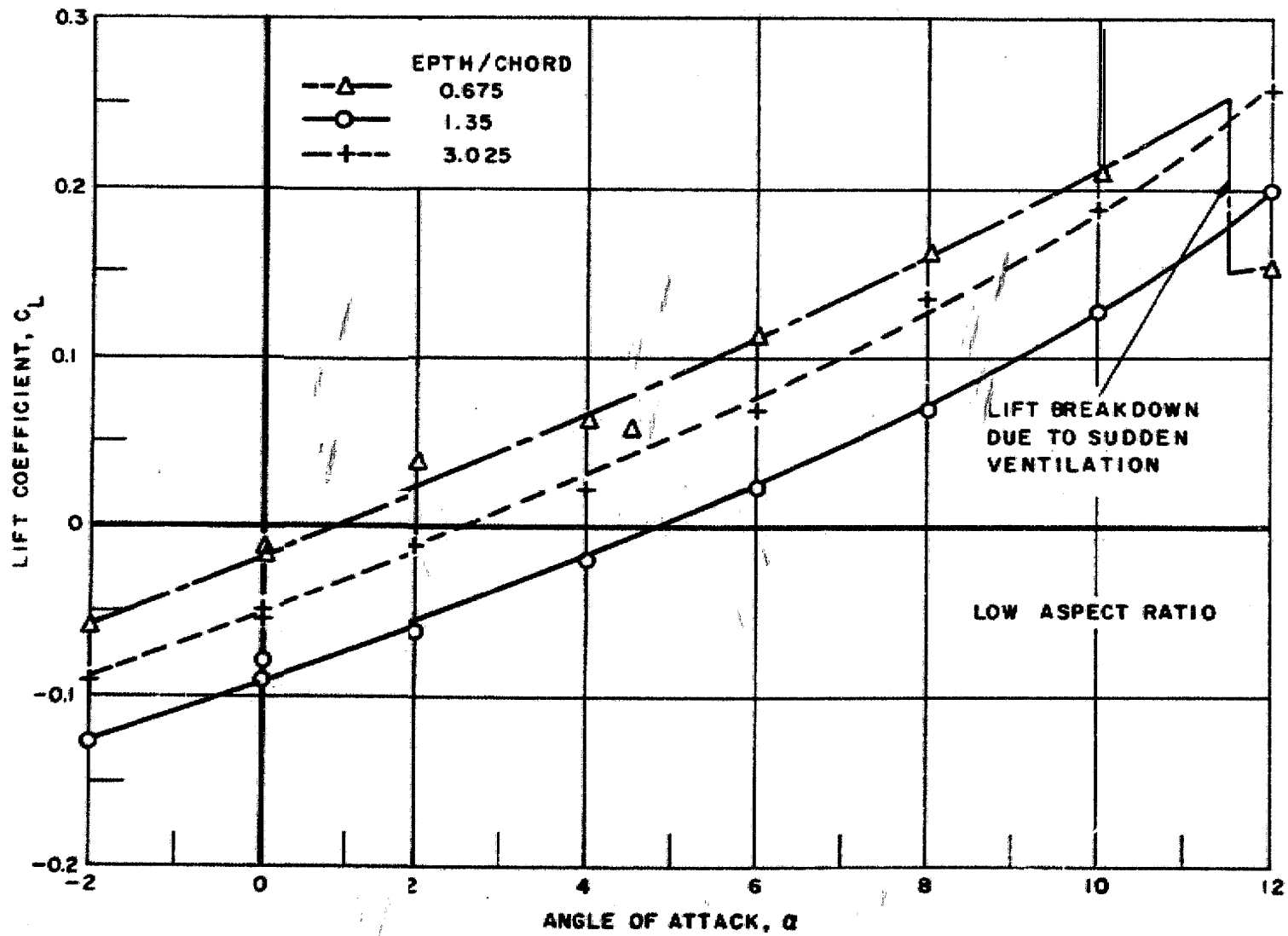
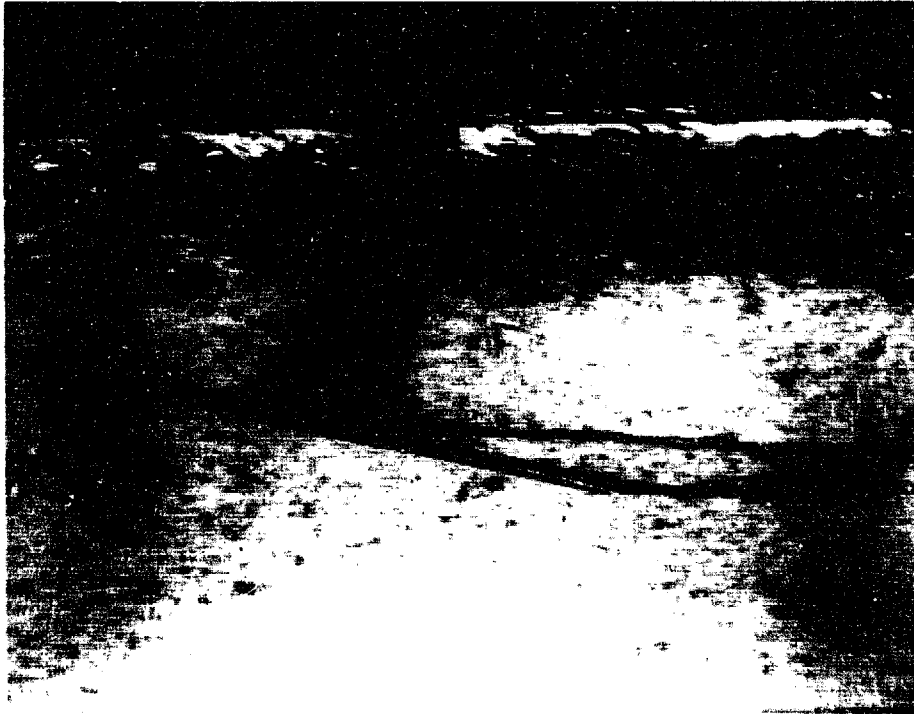


FIG. 7. EFFECT OF FOILDEPTH OF SUBMERGENCE ON LIFT. SWEEP ANGLE = 90 DEG, V=11.80 FT/SEC



(A) HIGH ASPECT RATIO, ATTACK ANGLE OF 10 DEG.,  
SPEED = 9.27 FT/SEC,  $\sigma = 1.41$



(B) LOW ASPECT RATIO, ATTACK ANGLE OF 13 DEG.,  
SPEED = 11.61 FT/SEC,  $\sigma = 0.90$

FIG. 8. ILLUSTRATING FLOW OVER HYDROFOIL, 2 INCH DEPTH OF SUBMERGENCE

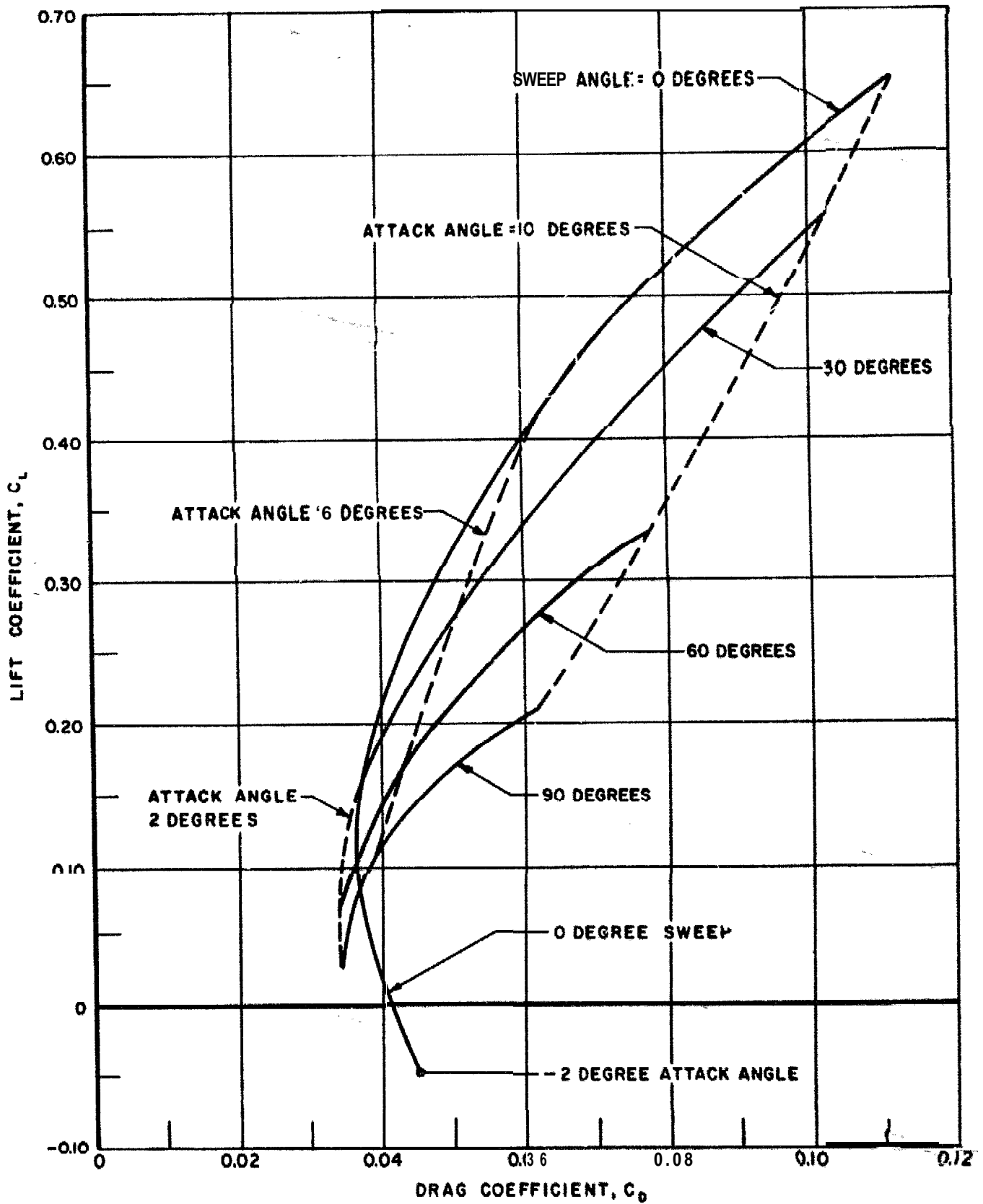
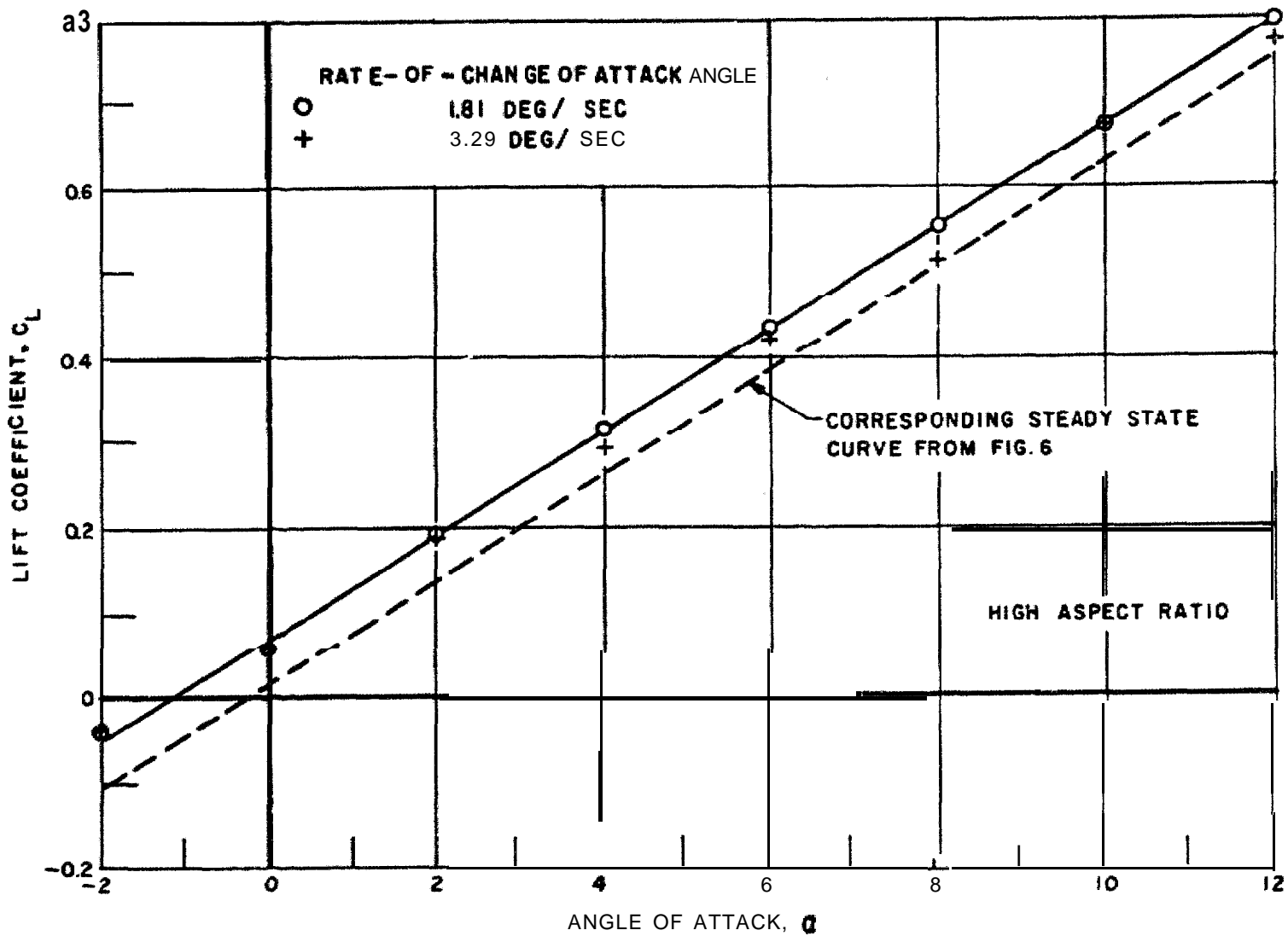


FIG. 9. LIFT COEFFICIENT VERSUS DRAG COEFFICIENT FOR VARIOUS SWEEP ANGLES AND ATTACK ANGLES, NOMINAL DEPTH/ MEAN CHORD RATIO = 0.675, CAVITATION INDEX = 0.908



LR-1332

FIG. 10. EFFECT OF UNSTEADINESS DUE TO CONTINUOUS VARIATION OF ANGLE OF ATTACK. SWEEP ANGLE = 0 DEG.,  $V=11.72$  FT/SEC, DEPTH/CHORD=1.35

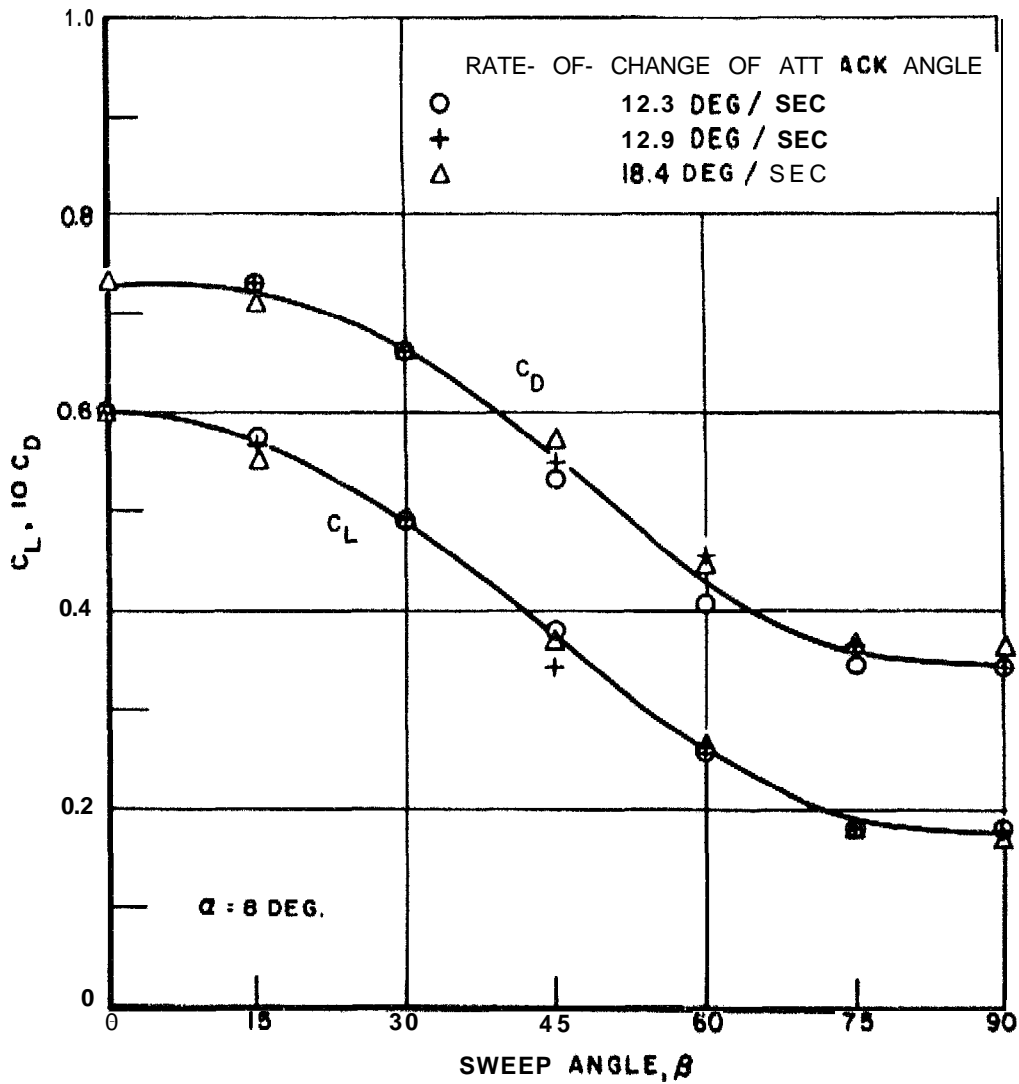


FIG. II. EFFECT OF UNSTEADINESS DUE TO CONTINUOUS VARIATION OF SWEEP ANGLE. ATTACK ANGLE=8 DEG,  $V= 11.72$  FT/SEC, DEPTH/CHORD= 1.35

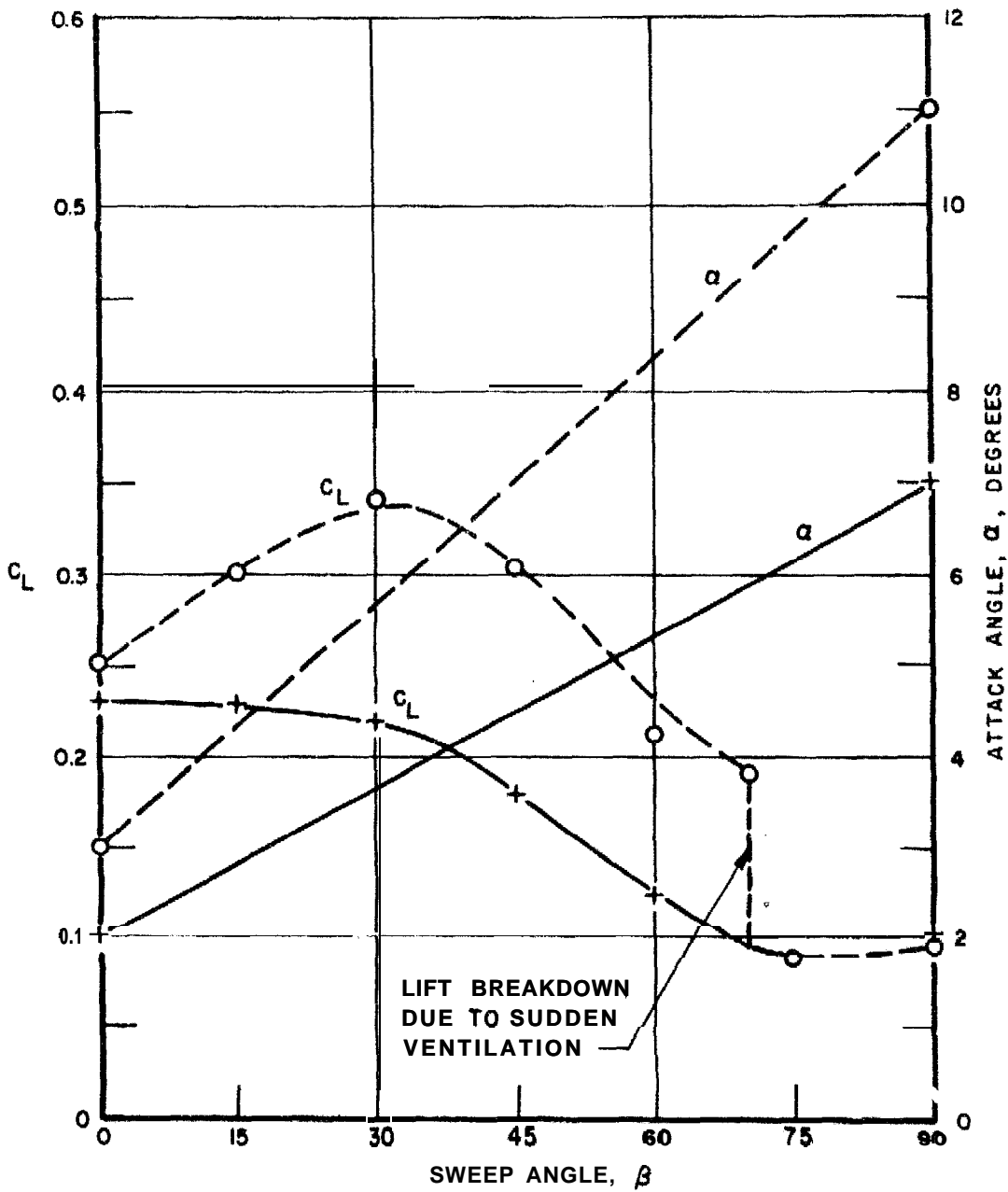
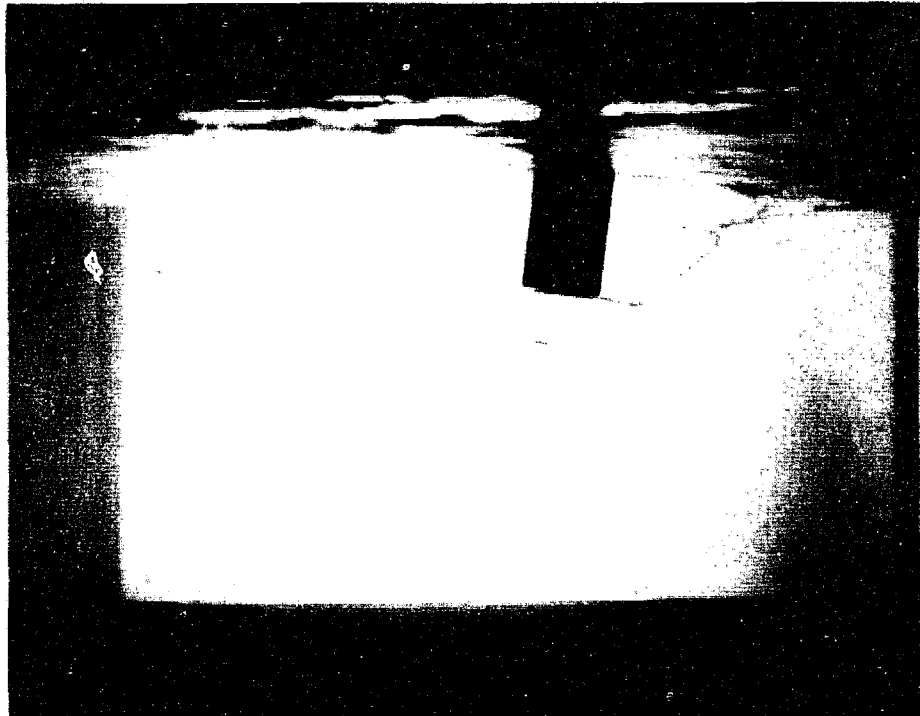
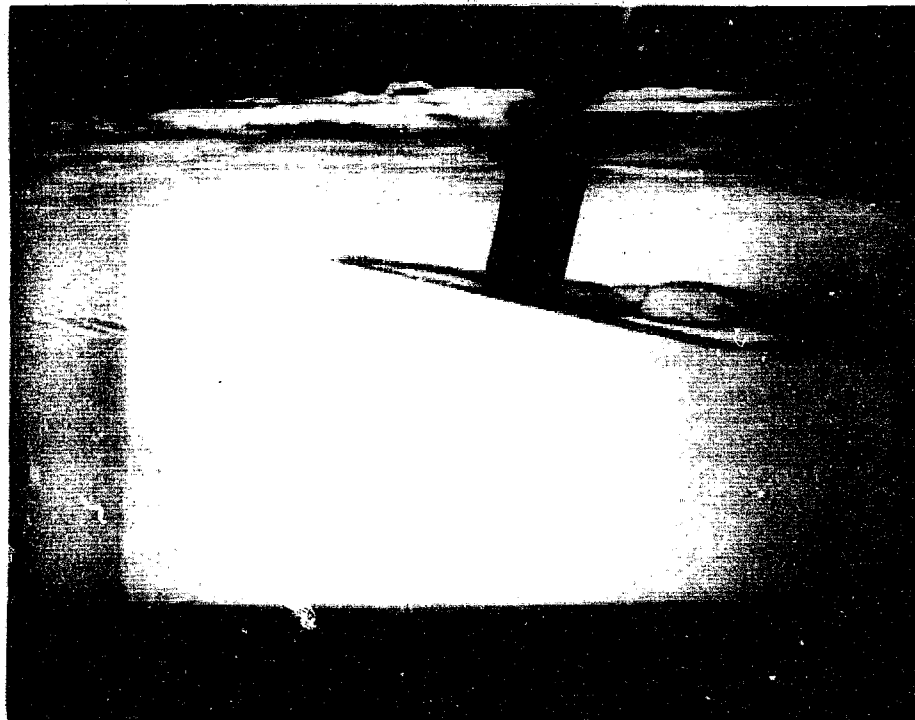


FIG. 12. EFFECT OF COMBINED ATTACK ANGLE AND SWEEP ANGLE VARIATIONS OF LIFT.  $V = 13.44$  FT/ SEC, DEPTH/CHORD = 0.675



(A) HIGH ASPECT RATIO, ATTACK ANGLE OF 7 DEG.,  
SPEED = 6.81 FT/SEC,  $\sigma = 2.55$   
NOTE "PINCHING - OFF" OF VENTILATED REGION BEHIND STRUT



(B) LOW ASPECT RATIO, ATTACK ANGLE OF 4 DEG.,  
SPEED = 12.45 FT/SEC,  $\sigma = 0.78$   
NOTE LARGE, SPIRALLING ROLL-UP VORTICES

FIG. 13. ILLUSTRATING FLOW OVER HYDROFOIL, 2 INCH DEPTH OF SUBMERGENCE

DAVIDSON LABORATORY, Stevens Inst. of Tech.  
Hoboken, N.J. 07030

TESTS OF A VARIABLE SWEEP HYDROFOIL WITH  
CAVITATION AND VENTILATION

Research Letter Report 1332. DL 3374/310. Final.

John A. Mercier. January 1969. v + 20 + 13 figures.

Contract N600(19)62908, Task Order 10.  
Prepared for the Department of the Navy.  
Naval Air Systems Command.

Distribution of this document is unlimited.

DAVIDSON LABORATORY, Stevens Inst. of Tech.  
Hoboken, N.J. 07030

TESTS OF A VARIABLE SWEEP HYDROFOIL WITH  
CAVITATION AND VENTILATION

Research Letter Report 1332. DL 3374/310. Final.

John A. Mercier. January 1969. v + 20 + 13 figures.

Contract N600(19)62908, Task Order 10.  
Prepared for the Department of the Navy.  
Naval Air Systems Command.

Distribution of this document is unlimited.

DAVIDSON LABORATORY, Stevens Inst. of Tech.  
Hoboken, N.J. 07030

TESTS OF A VARIABLE SWEEP HYDROFOIL WITH  
CAVITATION AND VENTILATION

Research Letter Report 1332. DL 3374/310. Final.

John A. Mercier. January 1969. v + 20 + 13 figures.

Contract N600(19)62908, Task Order 10.  
Prepared for the Department of the Navy.  
Naval Air Systems Command.

Distribution of this document is unlimited,

DAVIDSON LABORATORY, Stevens inst. of Tech.  
Hoboken, N.J. 07030

TESTS OF A VARIABLE SWEEP HYDROFOIL WITH  
CAVITATION AND VENTILATION

Research Letter Report 1332. DL 3374/310. Final.

John A. Mercier. January 1969. v + 20 + 13 figures

Contract N600(19)62908, Task Order 10.  
Prepared for the Department of the Navy,  
Naval Air Systems Command.

Distribution of this document is unlimited.

UNCLASSIFIED

Security Classification

DOCUMENT CONTROL DATA - R & D

(Security classification of title, body of abstract and indexing annotation must be entered when the overall report is classified)

1. ORIGINATING ACTIVITY (Corporate author) DAV I DSDN LABORATORY STEVENS INSTITUTE OF TECHNOLOGY CASTLE POINT STATION, HOBOKEN, N.J. 07030	2a. REPORT SECURITY CLASSIFICATION <b>UNCLASSIFIED</b>
	2b. GROUP

3. REPORT TITLE  
**TESTS OF A VARIABLE SWEEP HYDROFOIL WITH CAVITATION AND VENTILATION**

4. DESCRIPTIVE NOTES (Type of report and, inclusive dates)  
**FINAL**

5. AUTHOR(S) (First name, middle initial, last name)  
**JOHN A. MERCIER**

6. REPORT DATE <b>JANUARY 1969</b>	7a. TOTAL NO. OF PAGES <b>v+20+13 figures</b>	7b. NO. OF REFS <b>4</b>
---------------------------------------	--	-----------------------------

8a. CONTRACT OR GRANT NO. <b>N600(19)62908, Task Order 10</b> b. PROJECT NO. <b>DL 3374/3 10</b> c. d.	9a. ORIGINATOR'S REPORT NUMBER(S) <b>LETTER REPORT NO. 1332</b>
	9b. OTHER REPORT NO(S) (Any other numbers that may be assigned this report)

10. DISTRIBUTION STATEMENT  
**DISTRIBUTION OF THIS DOCUMENT IS UNLIMITED**

11. SUPPLEMENTARY NOTES	12. SPONSORING MILITARY ACTIVITY <b>DEPARTMENT OF THE NAVY NAVAL AIR SYSTEM3 COMMAND</b>
-------------------------	---

13. ABSTRACT

An experimental study of the performance of a variable sweep hydrofoil was carried out in the ~~Davidson Laboratory~~ variable pressure circulating water channel under conditions of reduced ambient pressure. A hydrofoil with tapered planform and typical sub-cavitating sections in the high aspect ratio (AR) attitude was attached to a base ventilated strut in such a way that it could be rotated, thus changing foil sweep. The attack angle of the foil and strut system were adjustable.

Measurements were made of the lift and drag acting on the foil and strut as a function of attack angle, sweep angle, depth of submergence and cavitation index for both steady foil position and with sweep and attack angles continuously varying. Still and motion picture records of some interesting flow phenomena were obtained.

14

KEY WORDS

LINK A

LINK B

LINK C

ROLE

WT

ROLE

WT

ROLE

WT

HYDROFOILS  
VARIABLE SWEEP